Nonlinear supercurrent response in anisotropic superconductors

Branko P. Stojković and Oriol T. Valls
School of Physics and Astronomy, University of Minnesota, Minneapolis, Minnesota 55455-0149
(Received 10 May 1994; revised manuscript received 2 August 1994)

We study the nonlinear supercurrent response of unconventional superconductors to an applied magnetic field. We calculate numerically the superconducting penetration depth λ and the magnetization component transverse to the applied magnetic field, at finite temperature and in arbitrary field, in the Meissner state. In the d-wave pairing state we find that both quantities exhibit nonlinear effects, due to the presence of nodes in the order parameter. We relate the results to various experimental situations and show how one can verify whether an observed $\lambda(T,H)$ is a signature of a particular pairing state. For an admixture of s-wave and d-wave superconducting states, we find that the transverse magnetization is suppressed, but that the s-wave component effect on the penetration depth may be overlooked in sufficiently large magnetic fields. We also consider dirty d-wave superconductors and discuss how these quantities, calculated as a function of temperature and field, are altered in this case.

I. INTRODUCTION

The discovery of high-temperature superconductors (HTSC's) (Ref. 1) has prompted a vast theoretical and experimental research effort aimed at the explanation of their peculiar properties. Although many experimental and theoretical results have been accumulated over the years, the mechanism of superconductivity in these materials remains a mystery. Moreover, even the symmetry of the order parameter (OP) in HTSC's, a knowledge of which would considerably narrow the field of possible theoretical models of high-T_c superconductivity, has not been unambiguously determined, and there is experimental evidence in favor of and against every proposed pairing state. The details of the pairing state may also have a bearing on technological applications, such as the realization of devices based on Josephson junctions.

Among the leading candidates for the pairing state, one must consider the spin-singlet $d_{x^2-y^2}$ pairing state ("d wave") with four nodal lines on the Fermi surface (FS) along which the OP vanishes. A state with d-wave symmetry might be taken as an indication that the superconductivity in HTSC's is mediated by an unconventional mechanism involving, e.g., antiferromagnetic spin fluctuations,[2] rather than phonons.[3] Several recent experimental results have been interpreted as a confirmation of the existence of this pairing state.[4] However, other experiments[5] and theoretical work[6] favor a conventional "s-wave" pairing state having the full point-group symmetry of the crystal lattice and no OP nodes. Thus the process of winnowing the competing theories is difficult due to the ambiguous experimental evidence.

These developments have renewed interest in the theory of the supercurrent response of superconductors with reduced symmetry pairing states, previously studied in the context of superfluid ^{3}He and heavy fermion superconductors.[7] Superconductors carrying a current have been studied extensively in the context of gapless superconductivity in thin films in a magnetic field.[8,9] This fully microscopic approach has been very useful in analyzing a variety of experiments in the past. However, nonlinear effects induced by moderate applied magnetic fields are negligible in bulk s-wave superconductors. This is not the case for unconventional superconductors, which exhibit a nonlinear Meissner effect: Yip and Sauls have recently argued[10] that the field dependence of the supercurrent response of a d-wave superconductor can be used to locate the positions of the nodal lines of the OP, since the anisotropy of the OP implies anisotropy of the response. Even though they only presented results for superconductors in small magnetic fields and at $T = 0$, experiments[11] based on these nonlinear effects at finite temperatures have already been performed. These experiments have prompted the present calculation.

In this paper we take up the computation of the nonlinear effects in the supercurrent response of anisotropic superconductors to an applied magnetic field at the experimentally relevant ranges of finite temperatures and larger magnetic fields (in the Meissner regime). We work within the framework originally presented in Ref. 10. Our main objective is to relate the nonlinear effects predicted by the theory to experimentally observable quantities. We focus on the superconducting penetration depth (or screening length) $\lambda(T,H)$ as a function of temperature and field, and on the transverse magnetic moment $\mathbf{m}_\perp$, that is, the component perpendicular to the applied magnetic field, which is present in superconductors with unconventional pairing state symmetries. We show how these quantities depend also on the angle ϑ between the applied field and the direction of the OP nodes, and calculate $\mathbf{m}_\perp$ as a function of this angle.

We discuss the ranges of field and temperature in which nonlinear effects should be experimentally observable in d-wave superconductors, and explain how one may verify whether recent penetration depth measurements are indeed a signature of d-wave superconductivity. We also investigate how the addition of a small s-wave component

to the pairing state ("$s+id$" state) affects the anisotropy of the supercurrent response and address other issues and problems related to the question of properly allowing for the possible existence of nonlinear effects interpreting experimental results. Finally, we briefly discuss the effect of impurities.

Our results can be summarized as follows: the nonlinear Meissner effect [i.e., nonlinear effects in $\lambda(T,H)$ and nonvanishing $\mathbf{m}_\perp$] should be observable in HTSC materials at low temperatures ($T \sim$ 1–10 K for moderate magnetic fields) if the pairing is pure d wave. A rather small admixture of s-wave pairing drastically reduces $\mathbf{m}_\perp$, while the d-wave character may still be apparent in $\lambda(T,H)$ at larger fields. On the other hand, $\mathbf{m}_\perp$ is less sensitive to impurities than the behavior of the penetration depth as a function of both field and temperature.

This paper is organized in the following way: in Sec. II we review the theoretical model used to calculate the transverse magnetization and the penetration depth of unconventional superconductors. Section III contains the discussion of our results and the conclusions regarding their experimental implications.

II. MODEL

In this section we discuss the methods we use to calculate the current response of unconventional superconductors from which we extract the physical quantities of interest. These methods are based on the formalism briefly described in Ref. 10, which we review here in some detail in order to explain our calculations. The formalism is based on the evaluation of the current field as initially addressed by Bardeen,[12] and later developed in terms of the quasiclassical transport equation.[13] We emphasize how the anisotropy of the response leads to a transverse magnetic moment, observable in experiments. We also show how one extracts the effective penetration depth as a function of the applied field.

We consider a superconductor infinite in the a-b plane and of thickness d in the c direction. We assume a coordinate system with its z axis parallel to the c crystallographic direction of the superconductor, and a topologically cylindrical Fermi surface, so that the problem is effectively two dimensional. As in Ref. 10 we define a superfluid "velocity" field:[14]

$$\mathbf{v} = \frac{\nabla\phi}{2} + \frac{e}{c}\mathbf{A}, \tag{2.1}$$

where ϕ is the phase of the superconducting order parameter, and $\mathbf{A}$ is the vector potential. It is easily confirmed[8] that the mass scale enters the theory only in the definition of the zero-temperature quantities, such as the zero-temperature penetration depth λ_0 defined below, and is otherwise unnecessary. Then in the Meissner phase, the supercurrent generated by the magnetic field is given by[10,12]

$$\mathbf{j} = -eN_f \int d\Omega\, n(\Omega)\, \mathbf{v}_f(\Omega) \left[\sigma(\Omega) + \int_0^\infty d\xi \frac{1}{2}\left(\tanh\frac{E-\sigma(\Omega)}{2T} - \tanh\frac{E+\sigma(\Omega)}{2T}\right)\right], \tag{2.2}$$

or alternatively, in terms of Matsubara frequencies $\omega_n = (2n+1)\pi T$:

$$\mathbf{j} = -eN_f \int d\Omega\, n(\Omega)\, \mathbf{v}_f(\Omega) \pi T \sum_n \frac{\sigma(\Omega) - i\omega_n}{\sqrt{[\omega_n + i\sigma(\Omega)]^2 + |\Delta(\Omega)|^2}}. \tag{2.3}$$

Here $\mathbf{v}_f$ is the quasiparticle velocity at the point Ω on the Fermi surface, $\sigma(\Omega) = \mathbf{v}_f(\Omega)\cdot\mathbf{v}$ is the quasiparticle energy shift due to the superflow, N_f is the total density of states at the Fermi surface, $n(\Omega)$ is the angle resolved density of states normalized to unity, $E = \sqrt{\xi^2 + |\Delta(\Omega)|^2}$, and T is the temperature. Equation (2.2) is numerically more convenient for clean systems at low nonzero temperatures. On the other hand, one must use Eq. (2.3) when considering the effects of impurities. The first term in Eq. (2.2) is the supercurrent response of the unperturbed condensate at $T = 0$, while the second term is due to the quasiparticles, formed by the pair breaking induced by the applied magnetic field and temperature.

One can, of course, consider conventional "s-wave" [$(\Delta(\Omega) = \Delta_S = \text{const}$] or unconventional order parameters. For the unconventional case, we assume that $\Delta(\Omega)$ has line nodes on the Fermi surface, defined by $|\hat{k}_x| = |\hat{k}_y|$, the so-called $d_{x^2-y^2}$ d-wave pairing state. Thus

$$\Delta(\hat{\mathbf{k}}) = \Delta_0 (\hat{k}_x^2 - \hat{k}_y^2) = \Delta_0 \cos(2\theta). \tag{2.4}$$

Here $\hat{\mathbf{k}}$ is a two-dimensional unit vector in momentum space and Δ_0 is the maximum value of $\Delta(\hat{\mathbf{k}})$. The temperature range we will consider is sufficiently below T_c that the T dependence of Δ_0 is unimportant.[2] We will also treat a "mixed" ($s+id$) state where we assume that the nodes of the d-wave part are shifted radially from the Fermi surface by a constant amount, equal to the s-wave component Δ_S of the pairing state.

From Eqs. (2.2) and (2.3) it is obvious that the supercurrent is a nonlinear and nontrivial function of the velocity field at any $T \neq 0$. As pointed out in Refs. 15 and 16, the current (2.2) is a nonanalytic function of temperature at $T = 0$. For conventional s-wave superconductors in the Meissner state, however, one has $\sigma(\Omega) \ll \Delta(\Omega)$ and, since the Fermi surface is symmetric, the two parts of the second term of Eq. (2.2) identically cancel each other at $T = 0$.

In the case of unconventional superconductors the sit-

uation is different: the order parameter of a d-wave superconductor changes sign under a $\pi/2$ rotation about the c axis, which implies a two-fold symmetry since $\Delta(\hat{k}) = \Delta(-\hat{k})$ for both the d and $(s+id)$-pairing states. This, however, produces a four-fold symmetry of the current since $|\Delta(\theta)|^2 \sim \cos^2(2\theta)$ in Eq. (2.2), i.e., $\mathbf{j}$ is insensitive to the sign of Δ. It is very important to realize that the current response, whether probed through direct measurements of the magnetic moment or by measuring the penetration depth, is insensitive to the phase of Δ and therefore cannot distinguish between the d-wave pairing state and a sufficiently anisotropic s-wave state with the same symmetry of $|\Delta|^2$.

The main difference between a superconductor with a full gap on the FS and a superconductor with nodes is, of course, in the excitation spectrum. Just as in the case of gapless superconductors, there are, in the unconventional case, single quasiparticle states available on the FS even at $T = 0$. These states are positioned near the nodes on the FS, which implies then that the potential energy of the system, as seen by the velocity field, has a four-fold symmetry. On the other hand, the velocity field is easily related to measurable quantities such as the magnetic moment $\mathbf{m}$. Therefore a measurement of the anisotropy of $\mathbf{m}$ may reveal the anisotropy of the current response which can then be used to determine the anisotropy of the gap. We shall further clarify this point shortly.

In order to calculate the magnetic moment and the supercurrent density of an unconventional superconductor, one must solve Eqs. (2.2) and (2.3) together with Maxwell's equations. The choice of gauge $\nabla \cdot \mathbf{v} = 0$ is the most convenient one since $\nabla \times \mathbf{H} = 4\pi\mathbf{j}/c$ reduces to

$$-\nabla^2 \mathbf{v} = \frac{4\pi e}{c^2}\mathbf{j}(\mathbf{v}). \tag{2.5}$$

In the slab geometry considered here and for magnetic fields $\mathbf{H}$ parallel to the slab interfaces, Ampère's law requires that the local magnetic field,

$$\mathbf{b} = \frac{c}{e}\nabla \times \mathbf{v}, \tag{2.6}$$

and the velocity field have only x and y components, which depend *only* on z, i.e., the distance from the boundaries.

We now make the assumption that the FS has a circular cross section, which simplifies the calculation. We will later show that this assumption is adequate. Defining then the dimensionless quantities,

$$\mathbf{V} = \frac{v_f}{\Delta_0}\mathbf{v}, \qquad \delta(\theta) = \frac{\Delta(\theta)}{\Delta_0}, \qquad t = \frac{T}{\Delta_0}, \tag{2.7}$$

Eqs. (2.2) and (2.5) reduce to

$$\lambda_0^2 \frac{d^2\mathbf{V}}{dz^2} = \mathbf{V} + \int \frac{d\theta}{2\pi}\hat{\mathbf{k}} \int d\xi \left[\tanh \frac{\sqrt{\xi^2 + |\delta(\theta)|^2} - \mathbf{V}\cdot\hat{\mathbf{k}}}{2t} - \tanh \frac{\sqrt{\xi^2 + |\delta(\theta)|^2} + \mathbf{V}\cdot\hat{\mathbf{k}}}{2t} \right], \tag{2.8}$$

with

$$\lambda_0^2 = \frac{c^2}{2\pi e^2 N_f v_f^2}. \tag{2.9}$$

Alternatively, one can derive an expression equivalent to (2.8), in terms of sums over Matsubara frequencies, from Eqs. (2.3) and (2.5). The above equations must be solved with a natural boundary condition,

$$\mathbf{b}\left(z = -\frac{d}{2}\right) = \mathbf{b}\left(z = \frac{d}{2}\right) = \mathbf{H}, \tag{2.10}$$

where d is the thickness of the slab or equivalently,

$$\mathbf{b}\left(z = \pm\frac{d}{2}\right) = \mathbf{H}, \quad \mathbf{v}(z = 0) \equiv 0. \tag{2.11}$$

Equation (2.8) cannot be solved exactly except for very small magnetic fields and at zero temperature where there are accurate approximate expansions.[10] For any nonzero temperature or at higher magnetic fields, the solution must be sought numerically. This issue is of extreme importance: as pointed out in Ref. 10 and in the next section, for the phenomena studied here a d-wave superconductor, in a typical experimental situation, is in the low-temperature regime only at temperatures of order of a few degrees Kelvin. This means that most of the "low-temperature" measurements,[17] involving the supercurrent response of HTSC's, are actually performed in a temperature range *higher* than that needed for observation of the *zero-temperature* behavior of these materials. Therefore, one cannot consider the zero-temperature solution of Eq. (2.8) as sufficient when analyzing experiments. We shall return to this question in Sec. III.

Numerically, the solution of (2.8) may be somewhat simplified by rewriting it in the form:

$$\frac{d^2\mathbf{V}}{dz^2} = -\nabla_V F(\mathbf{V}), \tag{2.12}$$

where $F(\mathbf{V})$ is a scalar function. From Eq. (2.8) one finds

$$F(\mathbf{V}) = \frac{1}{\lambda_0^2}\left\{ -\frac{1}{2}\mathbf{V}^2 + \frac{t}{\pi}\int d\theta \int d\xi \times \ln\left[1 + \sinh^2 \frac{\mathbf{V}\cdot\hat{\mathbf{k}}}{2t}\,\mathrm{sech}^2 \frac{\sqrt{\xi^2 + |\delta(\theta)|^2}}{2t} \right] \right\}. \tag{2.13}$$

Equation (2.12) is formally identical to that of a classical particle in a potential field and thus one has the first integral:

$$\frac{1}{2}\left(\frac{dV}{dz}\right)^2 + F(\mathbf{V}) = \text{const}\,, \tag{2.14}$$

where $V \equiv |\mathbf{V}|$. Notice, however, that in the presence

of nodes F is not a function of $|\mathbf{V}|$ only, which implies that $\hat{\mathbf{V}}$, the direction of the velocity field, is not a conserved quantity throughout the sample. This means that $d\mathbf{V}/dz$ is not parallel to $\mathbf{V}$, except at eight high symmetry points, i.e., gap nodes and antinodes. As a consequence, from Eqs. (2.5) and (2.10) it follows that the local magnetic field $\mathbf{b}$ is not parallel to the applied magnetic field $\mathbf{H}$ in the interior of the slab, and neither is the magnetic moment $\mathbf{m}$. Experimentally, this is the crucial point as an observation of $\mathbf{m}_\perp$, the component of the magnetic moment perpendicular to $\mathbf{H}$, reveals the anisotropy of $\Delta(\hat{\mathbf{k}})$.

The velocity field $\mathbf{V}(z)$, obtained by solving Eq. (2.8), can be straightforwardly used to calculate measurable quantities, such as the magnetic moment $\mathbf{m}$ (or equivalently the magnetization $\mathbf{M}$) and the effective penetration depth $\lambda(T,H)$. In particular, the penetration depth is defined as[10]

$$\frac{1}{\lambda(T,H)} = \frac{1}{H}\left|\frac{d\mathbf{b}}{dz}\right|_{z=\pm d/2}, \tag{2.15}$$

although alternative definitions are also applicable.[18] Since $\mathbf{b}$ and $\mathbf{H}$ are not parallel (except for the velocity field parallel to a node or antinode direction), the above definition is ϑ dependent.[10] In this paper we show λ only for the magnetic field applied along the nodes ($\vartheta = 0$) or the antinodes ($\vartheta = \pi/4$) of a superconductor, as discussed in Sec. III, and give the full dependence of $\mathbf{m}_\perp$ on ϑ.

The magnetic moment is[19]

$$\mathbf{m}(T,H) = \frac{1}{2c}\int_{-d/2}^{d/2} d\mathbf{r}'\,\mathbf{r}' \times \mathbf{j}\left[\mathbf{V}(z')\right]. \tag{2.16}$$

As discussed above, in general, $\mathbf{m}$ is not parallel to the applied field $\mathbf{H}$ and we can extract its transverse component $\mathbf{m}_\perp = \mathbf{m} - \mathbf{H}\,(\mathbf{H}\cdot\mathbf{m}/|\mathbf{H}|^2)$. Provided that $d \gg \lambda_0$, the definition (2.15) leads to results independent of d. The *transverse* magnetic moment is also independent of d. This can easily be seen by recalling that the field B, the average of $\mathbf{b}$ throughout the sample, is proportional to λ/d in a slab.[20] The nonzero $\mathbf{m}_\perp$ implies[10] that a d-wave superconductor placed in a parallel magnetic field will exhibit a torque, which will then tend to rotate the sample about the c axis. The direction of the torque will also exhibit a four-fold symmetry, i.e., the sign of the torque changes every time the velocity field passes through an antinode.

Numerically, the solution of Eq. (2.12) is straightforward provided one has an efficient way of evaluating the function F in Eq. (2.13). This is readily accomplished by calculating F on a grid of points at a given temperature or magnetic field and then interpolating for an arbitrary value of the argument. The accuracy of the numerical solution can be verified by confirming that Eq. (2.14) is satisfied throughout the entire sample.

III. RESULTS

In this section we present our results obtained using the method described in Sec. II. We first discuss the relevant temperature and field ranges for the nonlinear Meissner effect which we further emphasize by presenting our results for the penetration depth and the transverse magnetic moment of a pure d-wave superconductor. We give these quantities also as a function of the angle ϑ between the applied magnetic field and the order parameter node, and discuss various experimental aspects involving the nonlinear Meissner effect. We then consider $(s+id)$ pairing and show how the addition of a small isotropic gap to the d-wave state affects the results. Finally, we study the effects of impurities on these quantities.

There are several physical parameters in our model, but only their dimensionless ratios are necessary [see Eq. (2.7)]. For the velocity field, one specifies the boundary condition (2.10), which can be rewritten as

$$\left|\lambda_0\left(\frac{d\mathbf{V}}{dz}\right)_{z=\pm d/2}\right| = \frac{H}{H_0}. \tag{3.1}$$

Here H_0 is a characteristic magnetic field:

$$H_0 = \frac{\phi_0}{\pi^2\lambda_0\xi_0}, \tag{3.2}$$

where ϕ_0 is the flux quantum and $\xi_0 = v_f/\pi\Delta_0$ is the superconducting coherence length. The function $F(\mathbf{V})$ in Eq. (2.13) also depends on T/Δ_0. Hence the results of our calculation are functions only of H/H_0 and T/Δ_0. When discussing thin films we also include the parameter d/λ_0. However, most of the results presented are for the usual case where $d \gg \lambda_0$.

In interpreting our results, as given in terms of dimensionless ratios, it is useful to keep in mind at least rough estimates of the characteristic values of Δ_0 and H_0 in typical experimental situations. The size of Δ_0 in HTSC's is somewhat controversial. Several models of high-T_c superconductivity imply a rather large value of Δ_0/T_c,[2] while others assume more BCS-like values of this parameter.[6] If one assumed that HTSC's are in the d-wave state then the value of Δ_0 might be obtained from the linear Meissner regime of $\lambda(T)$,[4] since for a pure d-wave superconductor at low temperature and vanishing field[21]

$$\lambda(T) \simeq \lambda_0\,(1 + C\,T/\Delta_0) \tag{3.3}$$

(where $C = \ln 2$ for a circular FS), but the determination would be impeded by the uncertainty in λ_0, as discussed below. In general, a value of $\Delta_0 \approx 200$–400 K is likely to be adequate for HTSC's of the Y-Ba-Cu-O (YBCO) family.[11]

The situation for H_0 is more complicated since this quantity may be strongly dependent on the particular experimental geometry and hence cannot be generally calculated. One must consider the actual current paths and, if one wishes to compare our theoretical results with those found in experimental situations, one is seriously hampered by the small size and large penetration depth anisotropy of the samples actually used, in contrast with the infinite slab geometry considered here. In a finite sample return currents flow along the c axis as well as in the a-b plane. For the purposes of estimating H_0 from

Eq. (3.2) one may assume that $\xi_0 \simeq 15$ Å in YBCO. From the definition (2.9) it is clear that λ_0 reflects the electronic density of the entire system and therefore its effective value as introduced in H_0 must include a contribution from the current flow in the z direction, characterized by a penetration depth λ_c which in the YBCO family is $\lambda_c \gg \lambda_{ab}$. A detailed calculation of these size effects is extremely difficult and clearly beyond the scope of this work: a cylindrical FS implies an infinite effective mass in the z direction and hence a very large λ_c, which means that only a system infinite in the a-b plane can be treated by the methods used here and in Ref. 10. In Ref. 11, the use of a weighted average of λ_{ab} and λ_c in Eq. (3.2) was resorted to which led,[11] for the sample geometry studied there (which was typical of that of available crystals), to an estimate of H_0 in the region $H_0 \simeq 3000$–4000 G. As mentioned above, this should be considered only as a rough estimate, although we believe it to be reasonable, and results that depend on estimates should not be viewed without caution. Since, except for very thin films ($d \ll \lambda_0$), the effective value of λ_0 enters our calculations only through H_0, we will present our results in terms of the ratio H/H_0, and we emphasize that better estimates of H_0 for anisotropic superconductors can be obtained from experimental information on the crossover field introduced two paragraphs below. Comparison of our work with measurement should preferably include a value of H_0 determined from experimental information.

Next we discuss the range of field and temperature where the nonlinear effects are observable. We recall that the quasiparticle contribution to the current [second term in Eq. (2.2)] is due to an interplay of the temperature T and the energy of the states created by the velocity field near the nodes in the gap. This contribution, at a given temperature, will be highly influenced by the applied magnetic field, and the response to the field varies with temperature. At low T one can observe the nonlinear effects of the magnetic field in $\lambda(T)$ and the four-fold anisotropy of the magnetization in a d-wave superconductor, only if the applied field is large enough compared to some critical field $\tilde{H}(T)$. Alternatively, the temperature must be lower than some critical temperature $\tilde{T}(H)$ at constant H. At a sufficiently large temperature, or for a sufficiently small magnetic field, one is always in the linear regime and the anisotropy of the magnetization cannot be detected. This physical picture can be clarified by assuming a small velocity field and expanding the second term in Eq. (2.2) in terms of σ/T (low magnetic field, high-temperature expansion). Then one has

$$\mathbf{j} \simeq -eN_f \int d\Omega\, n(\Omega)\, \mathbf{v}_f(\Omega)\sigma(\Omega) \times \left(1 - \frac{1}{2T}\int_0^\infty d\xi\, \mathrm{sech}^2 \frac{E}{2T}\right). \tag{3.4}$$

Equation (3.4) can be rewritten as

$$\mathbf{j} = \rho_S\, \mathbf{v}, \tag{3.5}$$

where ρ_S is the superfluid density. One can easily show that ρ_S is a scalar, since the second (temperature dependent) term in Eq. (3.4) is a function of $\cos^2 2\theta$ only and any off-diagonal components would involve an angular integral of functions which vanish identically. This means that for a superconductor with a circular Fermi surface in the d-wave pairing state the superfluid *linear* response to a magnetic field is isotropic in the $x-y$ plane. As a result, for $\sigma \sim H(\Delta_0/H_0) \ll T$, one is in the low field regime where the nonlinear effects due to the applied magnetic field, including the transverse magnetization, are negligible.

We are then led to define a crossover field $\tilde{H}(T) \sim H_0(T/\Delta_0)$ *above* which the nonlinear effects become important, and alternatively a crossover temperature $\tilde{T}(H) \sim \Delta_0(H/H_0)$ *above* which the nonlinear effects are small. For a characteristic field $H_0 \sim 3000$ G (as estimated in the literature[11]) and[2] $\Delta_0 \sim 300$ K one finds $\tilde{H} \sim 10$ G at temperatures of order few degrees Kelvin or $\tilde{T} \sim 5$–10 K for an applied magnetic field $H \sim 100$ G.[10] Conversely, the experimental values of $\tilde{H}(T)$ (i.e., the field value at which nonlinear effects are first observed, see below) can provide an estimate of H_0. From the above argument it is clear that, in order to observe the nonlinear effects, one must be either at low temperature or in a high magnetic field. The latter is experimentally inconvenient since the field of the first flux entry is rather small for high-T_c superconductors.[11] Therefore it seems more feasible to perform the experiments at sufficiently low temperatures. In what follows we shall concentrate on these experimentally significant ranges of H and T. From an experimental point of view one need not rely on estimates of $\tilde{H}$ and $\tilde{T}$: following the procedures discussed later it is possible to consistently determine whether measurements are taken in the linear regime. A determination of $\tilde{H}(T)$ will then yield a determination of H_0 for the sample studied.

We begin with our results for the penetration depth. As discussed in Sec. II, the effective penetration depth of anisotropic superconductors in a magnetic field depends on the current orientation with respect to the nodes of the order parameter. Figure 1 shows the penetration depth λ in a pure d-wave superconductor as a function of T/Δ_0 for several values of the applied field H, assuming an applied field in the direction of a node ($\vartheta = 0$). The quantity plotted is

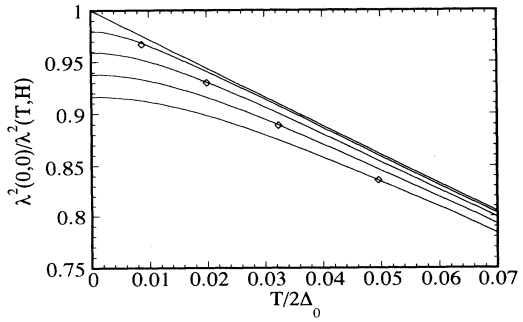

FIG. 1. Normalized penetration depth vs T/Δ_0, for (top to bottom) $H/H_0 = 0$, 0.03, 0.06, 0.09, 0.12. The diamonds indicate $\tilde{T}(H)$ as explained in the text. The field is applied in the direction of a line of nodes ($\vartheta = 0$).

$$\left[\frac{\lambda(T=0,H=0)}{\lambda(T,H)}\right]^2 \equiv \frac{n_S(T,H)}{n_S(0,0)}, \tag{3.6}$$

where

$$n_S(T,H) = \frac{mc^2}{4\pi e^2 \lambda^2(T,H)}. \tag{3.7}$$

All plots are normalized with respect to $\lambda_0 \equiv \lambda_0(T = 0, H = 0)$. It is important to realize that n_S includes the nonlinear effects and should *not* be confused with the superfluid density ρ_S defined in Eq. (3.5), which does not include such effects. The value of H increases from the top to the bottom curve (see caption). The topmost curve, corresponding to zero magnetic field, shows the well-known linear in T behavior (3.3). It is obvious that even for relatively low fields ($\sim$ 100 G with H_0 as estimated above) there is a deviation of $\lambda(T,H)$ from linearity in T at the temperatures where most low T experiments are performed. From the figure one can see that $\tilde{T}(H)$, identified as the temperature at which the deviation from linearity in T begins, and indicated by the diamond symbols,[22] is indeed of order $\Delta_0(H/H_0)$ which would mean of order $\sim$1–5 K at $H/H_0 \simeq 0.05$. On the other hand, for a sufficiently high temperature, $\lambda(T,H)$ is in its linear regime at all fields considered, and the slope of $n_S(T,H)$ is field independent as one can easily confirm from Eq. (3.5).

Experimentally, a linear dependence of $n_S(T,H)/n_S(0,0)$ on T has been reported.[4] This dependence would be, as claimed, evidence for d-wave pairing in the material studied (YBCO) provided that the experiment was done in the linear regime $T > \tilde{T}(H)$. Since the lowest temperatures studied were below 2 K, the effective fields used would have had to be below $\sim$10 G. It cannot be overemphasized that this type of restriction affects the analysis of virtually every experiment involving the electromagnetic response of HTSC's.

Turning now to the field dependence, we can easily see from Fig. 1 that, at constant T, $\lambda(H,T)$ has also two different regimes as a function of H. As shown analytically by Yip and Sauls,[10] $\lambda(0,H) - \lambda(0,0) \sim H/H_0$, while at higher temperatures $\lambda(T > \tilde{T}, H) - \lambda(T > \tilde{T}, 0) \sim (H/H_0)^2$ or alternatively

$$n_S(0,0) - n_S(0,H) \sim \frac{H}{H_0} \tag{3.8}$$

and

$$n_S(T > \tilde{T}, H) - n_s(T > \tilde{T}, H) \sim \left(\frac{H}{H_0}\right)^2. \tag{3.9}$$

This is extremely important in analyzing experimental data obtained, for example, by measuring the surface impedance of high-T_c materials, as the effective magnetic field in these experiments may be quite high.[23]

The nonlinear effects are largest if the current flows along the nodes (Fig. 1). Figure 2 shows the same quantity as in Fig. 1 for the case where the applied field and the current flow are along the antinodes. Clearly, the predicted nonlinear effects are somewhat reduced and we find that

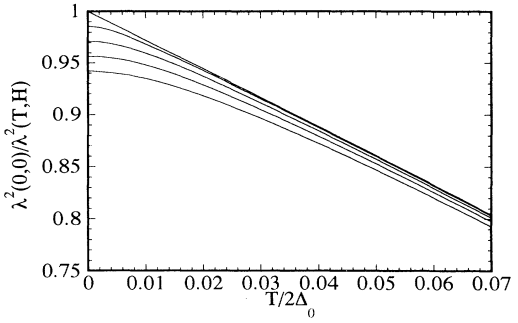

FIG. 2. As in Fig. 1, but with the applied field along a line of antinodes ($\vartheta = \pi/4$).

$$[n_S(0,0) - n_S(0,H)]_{\vartheta=0} \approx \sqrt{2}[n_S(0,0) - n_S(0,H)]_{\vartheta=\pi/4} \tag{3.10}$$

in harmony with previous predictions.[10] As expected from our discussion of Eq. (3.4), the zero field behavior of $\lambda(T,H)$ is exactly the same in both cases. This a-b plane anisotropy of the field-induced nonlinear behavior of $\lambda(T,H)$ appears to be rather large and should be observable in experiments on clean single crystals of, e.g., YBCO.

It is important to verify whether experimental results for $\lambda(T,H)$ are in the linear regime. This can be checked by measuring λ as a function of the applied magnetic field. For example, an approximately quadratic behavior $\lambda(T) - \lambda(0) \sim T^2$ might be consistent with a pure d-wave pairing state, provided one is in the region where $T \leq \tilde{T}$, which can be confirmed by verifying that $\lambda(H) \sim H$ in that temperature region and for the fields of the same order. Similarly, a $\lambda(T)$ linear in T should be checked as a function of H (e.g., by varying the applied power) to verify that Eq. (3.9) holds.

It is interesting to investigate the effect of the FS anisotropy on the results for $\lambda(T,H)$, and in particular on $\tilde{T}(H)$. In other words, it is important to clarify whether a more realistic form of the FS would significantly alter the crossover temperature. Enough information[24] is available on the FS of, e.g., YBCO in the k_x, k_y plane to make a discussion of this point possible. For the purposes of our analysis we assume a single tight-binding band of the form

$$\varepsilon(\mathbf{k}) = 2t - t(\cos k_x a + \cos k_y b), \tag{3.11}$$

where a and b are the lattice constants, and t is the bandwidth parameter. The FS is then given by $\varepsilon_F = (2-\delta)\,t$ and we assume $\delta = 0.1$ so that the FS has a shape similar to one of the branches depicted in Ref. 24. We then repeat the evaluation of $\lambda^2(0,0)/\lambda^2(T,H)$ assuming a velocity field along the a axis. The calculation is nearly identical to that in the previous section, except that v_F (and hence λ_0 and H_0) is redefined in terms of the new parameters. The results for $H/H_0 = 0.12$ are shown in

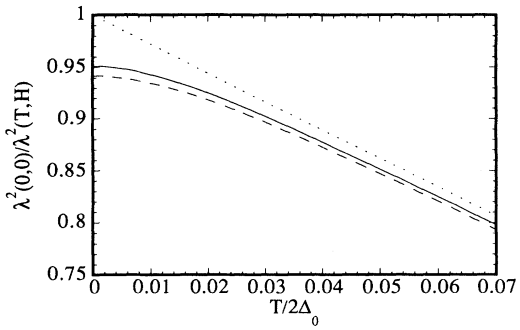

FIG. 3. Effect of FS anisotropy: the dashed line is the $H/H_0 = 0.12$ result of Fig. 2. The solid line is the corresponding result for a more realistic anisotropic FS (see text). The dotted line is the zero field result, as explained in the text.

Fig. 3 (solid line), and compared with the corresponding circular FS results (dashed line) of Fig. 2. Since the slope of the zero field result for the tight binding band is slightly different (by $\sim 7\%$) from the coefficient $\ln 2$ in Eq. (3.3), computed for a circular FS, we have slightly adjusted the horizontal scale, in plotting the solid lines, so that the zero field results (dotted line) coincide. Physically, this amounts to ensuring that we are comparing systems with the same T_c. Clearly, the two sets of curves are very similar and $\tilde{T}(H)$ is only marginally different, which is confirmed by an analysis such as that performed in Fig. 1. Thus our assumption of a circular FS is adequate.

The nonlinear Meissner effect is more prominent if the thickness of the sample is much larger than λ_0. Figure 4 shows the same quantity as in Fig. 1 for $d/\lambda_0 = 1$ (solid lines) and for $d/\lambda_0 \gg 1$ (dashed lines) at $H = 0$ (straight lines) and $H/H_0 = 0.12$ (lower curves) as would be seen in a surface impedance measurement. Here each $n_S(T,H)$ is normalized with respect to $n_S(0,0)$ for the same thickness. Clearly, there is a weaker nonlinear contribution in the case of thin film samples. Thinner samples may be more desirable for the (longitudinal) magnetization measurements, since their field of first flux entry is higher than in thick samples and the magnetization is a strong function of $\lambda(T,H)$. However, this type of experiment is difficult, as any vortex nucleation or sample tilt would lead to spurious nonlinear effects.

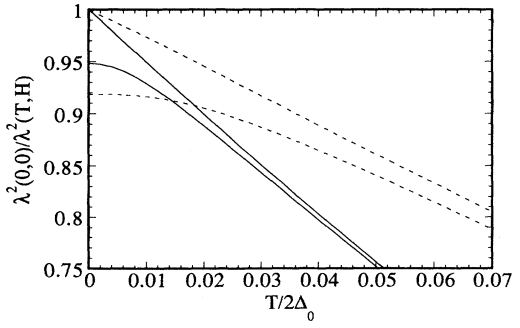

FIG. 4. Normalized penetration depth for $d \gg \lambda_0$ (dashed lines) and for $d = \lambda_0$ (solid lines), for the field direction as in Fig. 1. The straight lines are for $H = 0$ and the curves are for $H/H_0 = 0.12$.

A more direct way of probing the order parameter symmetry is through transverse magnetization measurements. Figure 5 shows the quantity $M_\perp$, defined as the magnitude of the transverse magnetic moment per unit area, at low temperature $t \equiv T/\Delta_0 = 0.005$, as a function of the angle ϑ. We only show one-eighth of a full circle which is sufficient because of the four-fold symmetry of $|\Delta(\theta)|^2$. The amplitude of $M_\perp$ is obviously zero along the lines of high symmetry, i.e., gap nodes (here shown at 0°) and antinodes (45°). At zero temperature and small magnetic field the transverse magnetic moment as a function of angle obeys[10]

$$M_\perp(\vartheta) \sim \sin\vartheta\cos\vartheta\,(\cos\vartheta - \sin\vartheta), \quad 0 < \vartheta < \pi/4, \tag{3.12}$$

which shows that $M_\perp(\vartheta)$ has a maximum, $M_\perp^0$, approximately at 21° with respect to a node. Our numerical results indicate that the local maximum position is very weakly dependent on temperature and field. At $T = 0$ the amplitude $M_\perp^0$ is proportional to H^2 to first order in H/H_0, while at higher temperatures $T > \tilde{T}$ we have $M_\perp^0 \sim H^3$. In Fig. 5 we find that $M_\perp^0 \sim H^{2.2}$, showing that $t \equiv T/\Delta_0 = 0.005$ is in the low-temperature regime.

At higher temperatures the quasiparticle flow becomes more isotropic, reducing the amplitude of $M_\perp$ and shifting its maximum towards 22.5°, measured from a node. Figure 6 shows the amplitude of $M_\perp$ as a function of temperature at a constant applied field $H/H_0 = 0.086$. Again, one can identify $\tilde{T}$ as the point where the sign of the curvature changes as the temperature is lowered. Besides its crossover from H^2 to the H^3 behavior, the amplitude of the transverse magnetization obviously decreases rapidly with increased temperature.

In an actual experiment[11] one rotates a sample about its c axis and searches for a component of the transverse magnetization with periodicity $\pi/2$. The amplitude of $M_\perp$ due to a d-wave pairing state is small even at $T = 0$ and is hard to observe for nontrivial sample geometries where it may be obstructed by the demagnetization

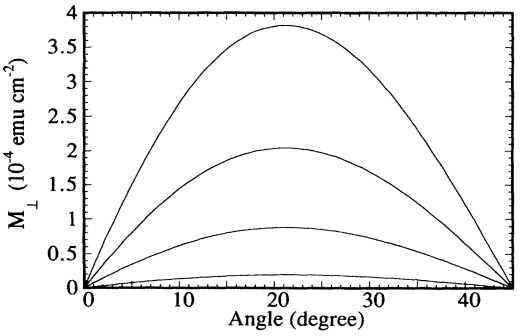

FIG. 5. The quantity $M_\perp$, defined as the magnitude of the transverse magnetic moment per unit area, vs the angle ϑ between **H** and a node position. The temperature is $T/\Delta_0 = 0.005$ and the field values (top to bottom) are $H/H_0 = 0.12, 0.09, 0.06, 0.03$.

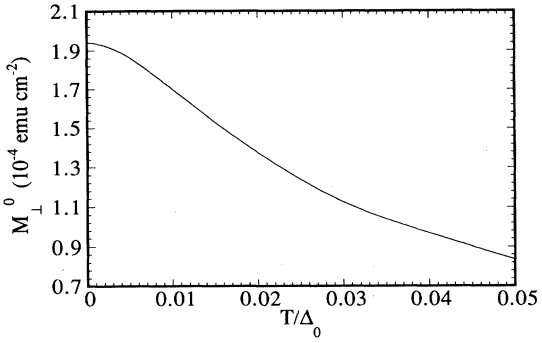

FIG. 6. The amplitude $M_\perp^0$ as a function of T/Δ_0 for $H/H_0 = 0.086$.

field, and by the orthorhombic crystal structure of high-T_c superconductors (Ref. 25): Although these produce $M_\perp$ signals with periodicity π, rather than $\pi/2$, they may have higher harmonics, giving a spurious $\pi/2$ signal. Moreover, the higher harmonics arising from even a small amount of trapped flux may have to be contended with. Disk shaped samples appear to be most favorable for this type of measurement since both the amount of trapped flux and the demagnetization effects should be minimized. It is also important to recall that the spurious signals will have a T and H dependence different from the distinctive d-wave behavior discussed here.

A recent transverse magnetization study of Buan *et al.*,[11] performed on an untwinned single crystal of $LuBa_2Cu_3O_{7-\delta}$, revealed no evidence of nodes in the pairing state: the results were inconsistent with a pure d-wave pairing state. This conclusion, however, assumed the previously mentioned estimate of H_0. A mixed $(s+id)$-pairing state has been proposed in the context of spin-fluctuations induced superconductivity with so-called "three-site states" included.[26] It was found that even a small amount of oxygen depletion leads to an addition of a small gap over the entire Fermi surface (s-wave component).[26] We have considered the $(s+id)$ state by repeating the calculation of $M_\perp$ and λ for a pairing state

$$\Delta(\hat{\mathbf{k}}) = \Delta_S + i\Delta_d(\hat{k}_x^2 - \hat{k}_y^2) \ , \tag{3.13}$$

with

$$|\Delta_S|^2 + |\Delta_d|^2 = |\Delta_0|^2. \tag{3.14}$$

It is straightforward to obtain results as a function of the additional parameter Δ_S/Δ_0. We find that the presence of Δ_S is very effective in suppressing $M_\perp$ as there is no creation of quasiparticles for applied fields smaller that $H_{\min} \sim H_0|\Delta_S/\Delta_0|$ at $T = 0$. For the experimental situation of Ref. 11 we find, assuming that $H_{\min}$ is the first flux entry field,[11] and accepting the value of H_0 as estimated in that work, that an s-wave component of 10–20% of the maximum order parameter is sufficient to suppress the transverse magnetization due to the presence of the d-wave component.

Similarly, a small s-wave component in the pairing state has a strong but less drastic effect on the nonlinear behavior of the penetration depth as a function of temperature. Figure 7 shows the same quantity with the same normalization as in Fig. 1, with the field applied along a line of nodes of the d-wave component. For $H \ll H_{\min}$ there is a crossover between the s-wave exponential behavior of $n_s(T,0)$ and the d-wave linear behavior at higher temperatures. The crossover temperature T^* is given, as expected, by $(\Delta_S/T^*)^{1/2}\exp(-\Delta_S/T^*) \sim 1/2\pi$. In a larger magnetic field the crossover temperature is reduced as the s-wave energy scale is lowered by the superflow as shown by the lowermost curve in Fig. 7. In fact, when $H \sim H_{\min}$ we find that $T^* \to 0$ and $n_S(T,H)$ looks essentially d-wave-like. Thus one might misinterpret the low-temperature linear $\lambda(T)$ in a magnetic field as being d wave, while lower fields would show an s-wave component.

Finally, we briefly present some results on the influence of impurities on the nonlinear Meissner effect in d-wave superconductors. We include the quasiparticle scattering due to impurities using standard perturbation techniques.[27] This effectively amounts only to replacing the Matsubara frequencies ω_n in Eq. (2.3) by the quantity $\tilde{\omega}_n$, obtained by solving the equation

$$\omega_n = \tilde{\omega}_n \left(1 - \frac{1}{2\tau}\frac{1}{\sqrt{\tilde{\omega}_n^2 + |\Delta(\theta)|^2}}\right), \tag{3.15}$$

where τ is the impurity scattering rate, calculated in the Born approximation. This procedure is formally equivalent to that of Abrikosov *et al.* in their treatment of magnetic (spin-flip) impurities,[8] although the physical picture here is quite different as the pair breaking is driven by the current. Then λ and $M_\perp$ are obtained in the same way as in the clean case.

The role of impurities in HTSC's is not well understood, since it has been found experimentally that even large scatterer concentrations cause only moderate reductions of the transition temperature. This in turn suggests that the Born approximation may not be adequate for small ξ_0 d-wave superconductors for which all impurities are pair breaking. Thus the results we present here are merely indicative of the general trends.

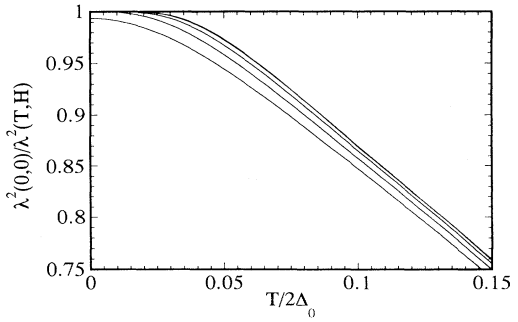

FIG. 7. The quantity plotted in Fig. 1 at field values $H/H_0 = 0$, 0.06, 0.09, 0.12, with an s-wave component $\Delta_S = 0.1\,\Delta_0$ (see text). The curve for $H/H_0 = 0.03$ is indistinguishable from that at $H = 0$.

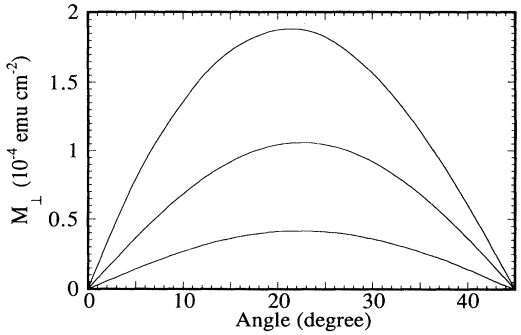

FIG. 8. $M_\perp$ vs ϑ for $H/H_0 = 0.086$ in the presence of impurities. From top to bottom $T_c/T_c^0 = 1$, 0.93, and 0.77.

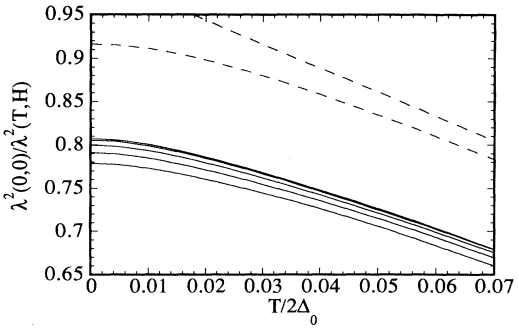

FIG. 9. The solid lines are as in Fig. 1, but for $T_c/T_c^0 = 0.93$. The normalization $\lambda_C(0,0)$ is as calculated in the clean case. The clean limit results at $H = 0$ and at $H/H_0 = 0.12$ are replotted here for comparison (dashed lines).

In the Born approximation the impurity scattering is characterized by the parameter $\tau\Delta_0$. However, since this parameter is not readily available in experiments on HTSC's, it is more practical to express the effect of impurities in terms of the transition temperature T_c. A recent self-consistent study[28] showed that T_c is a linear function of the scattering rate τ in a d-wave superconductor when the impurity concentrations are small. This dependence is quite similar to the behavior of s-wave superconductors in the presence of magnetic (pair-breaking) impurities,[8] when treated in the Born approximation. In the case of d-wave superconductors in the low impurity concentration limit, it holds for both Born and resonant scattering.[28] We use the results of Ref. 28 to estimate $\tau\Delta_0$ for several values of T_c/T_c^0, where T_c^0 is the transition temperature of a clean sample. In doing so we must make a choice for the ratio Δ_0/T_c^0, which is nontrivial, as explained at the beginning of this section. In the following we shall assume that $\Delta_0/T_c^0 = 3$, which is very reasonable considering the full range of this parameter in, e.g., YBCO family ($\Delta_0 \approx 200$–400 K and $T_c^0 \approx 93$ K).

Figure 8 shows the transverse magnetic moment per unit area as a function of angle for a d-wave superconductor in a constant magnetic field of $H = 0.086H_0$, for $T_c/T_c^0 = 1$, 0.93, and 0.77 (top to bottom). The magnetic moment is normalized in the same way as in Fig. 5. The impurities smear out the anisotropy of the response and the amplitude of $M_\perp$ is reduced. However, it is clear that only large values of the impurity self-energy Γ ($\Gamma \sim \Delta_0$) significantly reduce the transverse magnetic moment, and that the presence of impurities should not impede the observation of the nonlinear Meissner effect.

It has been recently found that only large amounts of scattering, in the Born approximation, can affect the temperature behavior of $\lambda(T, H = 0)$, but even small impurity concentrations in the unitary limit produce significant residual resistivity.[21] The penetration depth of dirty d-wave superconductors in finite applied magnetic field has not yet been considered. In Figure 9 we show the same quantity as in Fig. 1 for several values of the applied magnetic field and $T_c/T_c^0 = 0.93$ (moderately dirty sample). The results are normalized with respect to $\lambda_C(0,0)$, as calculated in the clean case. As expected, the quantity plotted deviates from linearity below a crossover temperature proportional to the impurity concentration, and then assumes a well-known quadratic low T behavior.[21] However, unlike in the clean case shown in Fig. 1, the result is only a weak function of the magnetic field, consistent with the claim that the impurities make the current response more isotropic. Similar to what was indicated below (3.10) in connection with the linear regime, it is also important to experimentally verify whether one is in the clean or dirty limit. The lack of field dependence in $\lambda(T, H)$ identifies the dirty limit.

In conclusion, we have performed a study of the applied magnetic field effect on the current response of unconventional superconductors (nonlinear Meissner effect). We find that the nonlinear effects can be very important and that they may considerably influence the interpretation of experimental results: in order to draw conclusions regarding the pairing state symmetry of HTSC's one must be extremely careful, as many experimental findings may be easily misinterpreted. We have indicated some of the checks that can be performed in order to verify the conclusions of an experimental analysis.

Our theory is not without limitations: an obvious qualm is that they are obtained for an infinite two-dimensional sample, with a cylindrical FS. In an actual finite sample currents flow in the z direction and the finite value of λ_c must be taken into account. These and other questions we plan to address in future work.

ACKNOWLEDGMENTS

We express our gratitude to A. Basovich, J. Buan, M. Friesen, R. Gianetta, A. M. Goldman, C. C. Huang, N. Israeloff, R. Joynt, R. Klemm, A. Leggett, B. H. Miller, D. Pines, J. Sauls, G. Spalding, and D. Van Harlingen for stimulating discussions on this problem, and S. A. Stojković and I. Žutić for careful reading of the manuscript. We thank the Minnesota Supercomputer Institute for a grant of computer time. One of us (B.P.S.) acknowledges the support of the U.S. Department of Education.

[1] J. G. Bednorz and K. A. Müller, Z. Phys. B **64**, 189 (1986).
[2] See, e.g., P. Monthoux, A. V. Balatsky, and D. Pines, Phys. Rev. Lett. **67**, 3448 (1991).
[3] J. Bardeen, L. N. Cooper, and J. R. Schrieffer, Phys. Rev. **108**, 1175 (1957).
[4] W. N. Hardy, D. A. Bonn, D. C. Morgan, R. Liang, and K. Zhang, Phys. Rev. Lett. **70**, 3999 (1993).
[5] See, e.g., P. Chaudhari and Shawn-Yu Lin, Phys. Rev. Lett. **72**, 1084 (1994).
[6] See, e.g., S. Chakravarty, A. Sudbø, P. W. Anderson, and S. Strong, Science **261**, 331 (1993).
[7] See P. W. Anderson and W. F. Brinkman, in *The Physics of Liquid and Solid Helium, Vol. II*, edited by K. H. Bennemann and J. B. Ketterson (Wiley, New York, 1978).
[8] K. Maki, in *Superconductivity*, edited by R. Parks (Dekker, New York, 1968).
[9] J. Bardeen, Rev. Mod. Phys. **34**, 667 (1962).
[10] S. K. Yip and J. A. Sauls, Phys. Rev. Lett. **69**, 2264 (1992).
[11] J. Buan, B. P. Stojković, N. E. Israeloff, A. M. Goldman, C. C. Huang, O. T. Valls, J. Z. Liu, and R. Shelton, Phys. Rev. Lett. **72**, 2632 (1994).
[12] J. Bardeen, Phys. Rev. Lett. **1**, 399 (1958).
[13] G. Eilenberger, Z. Phys **214**, 195 (1968); A. Larkin and Y. Ovchinnikov, Sov. Phys. JETP **28**, 1200 (1969); G. Eliashberg, *ibid.* **34**, 668 (1972).
[14] This expression for the superfluid velocity is appropriate for both s-wave states and for the d-wave pairing states proposed for HTSC's, which belong to a one-dimensional representation. Therefore, there are no additional contributions from internal degrees of freedom. See, for example, P. W. Anderson and W. F. Brinkman, in *The Physics of Liquid and Solid Helium, Vol. II*, edited by K. H. Bennemann and J. B. Ketterson (Ref. 7), p. 260.
[15] G. E. Volovik and V. P. Mineev, Sov. Phys. JETP **54**, 524 (1981).
[16] P. Muzikar and D. Rainer, Phys. Rev. B **27**, 4243 (1983).
[17] S. Sridhar, D.-H. Wu, and W. Kennedy, Phys. Rev. Lett. **63**, 1873 (1989).
[18] See R. Meservey and B. B. Schwartz, in *Superconductivity*, edited by R. D. Parks (Dekker, New York, 1969).
[19] J. D. Jackson, *Classical Electrodynamics* (Wiley, New York, 1975), p. 181.
[20] A. L. Fetter and J. D. Walecka, *Quantum Theory of Many Particle Systems* (McGraw-Hill, New York, 1971), p. 423.
[21] P. J. Hirschfeld and N. Goldenfeld, Phys. Rev. B **48**, 4219 (1993).
[22] The position of the diamond symbols is determined by fitting the curves to the asymptotic form $\sim a - bT^2/(\tilde{T}+T)$.
[23] E. K. Moser, W. J. Tomasch, M. J. McClorey, J. K. Furdyna, M. W. Coffey, C. L. Pettiette-Hall, and S. M. Schwarzbek, Phys. Rev. B **49**, 4199 (1994).
[24] O. K. Andersen, O. Jepsen, A. I. Lichtenstein, and I. I. Mazin, Phys. Rev. B **49**, 4145 (1994).
[25] J. Buan, B. Zhou, C. C. Huang, J. Z. Liu, and R. Shelton, Phys. Rev. B **49**, 12 220 (1994).
[26] Q. P. Li and R. Joynt, Phys. Rev. B **47**, 530 (1993); **48**, 437 (1993).
[27] A. A. Abrikosov, L. P. Gor'kov, and I. E. Dzyaloshinski, *Methods of Quantum Field Theory in Statistical Physics* (Dover, New York, 1975).
[28] P. Arberg and J. P. Carbotte, Phys. Rev. B **50**, 3250 (1994); P. Arberg, M. Manzor, and J. P. Carbotte, J. Phys. Chem. Solids **54**, 1461 (1993).